Sattler, A.; Paccagnini, M.; Liu, L.; Gomez, E.; Klutse, H.; Burton, AW.; Corma Canós, A. (2021). Assessment of metal-metal interactions and catalytic behavior in platinum-tin bimetallic subnanometric clusters by using reactive characterizations. Journal of Catalysis. 404:393-399. https://doi.org/10.1016/j.jcat.2021.10.006

Assessment of Metal–Metal Interactions and Catalytic Behavior in Platinum–Tin Bimetallic Subnanometric Clusters by Using Reactive Characterizations

Aaron Sattler*, Michele Paccagnini, Lichen Liu, Elaine Gomez, Henry Klutse, Allen W. Burton, Avelino Corma*

ABSTRACT

Several reactive characterizations were used to study the effect that reduction time has on propane catalysis using PtSn-K/MFI, including propane dehydrogenation, propane hydrogenolysis, and ethane H/D exchange. Propane dehydrogenation results demonstrate that increased reduction time causes the PtSn-K/MFI to have higher selectivity towards propylene, lower rates of catalyst deactivation, and lower rates of dehydrogenation. Consistent with higher selectivity towards propylene with longer catalyst reduction times, slower rates of hydrogenolysis are also observed over a large range of H_2:propane ratios. H/D exchange experiments to assess rates of C–H activation were carried out on PtSn-K/MFI by using ethane and D_2, which demonstrated that longer reduction time significantly inhibits the rate of C–H activation on PtSn-K/MFI. The substantial effects observed by using reactive characterizations were difficult to be interpreted by more advanced characterization techniques such as EXAFS, because the structural changes of the PtSn nanoclusters are quite subtle. Indeed, in a previous report on the PtSn-K/MFI material, Pt and Sn EXAFS were statistically indistinguishable with different reduction temperatures, illustrating that combining reactive characterizations, particularly with the application of H/D exchange, provides the ability to differentiate fundamental effects that impact catalyst performance. The importance of C–H activation was confirmed by isotopic experiments for propane dehydrogenation, which indicate that the first C–H activation step is rate-limiting during dehydrogenation, with a kinetic isotope effect of ~2.5. These results together show that increased reduction time gives a catalytic material with superior catalytic properties (i.e. higher propylene selectivity and lower deactivation rates), and this is proposed to be due to increased platinum-tin interactions, which modifies and weakens hydrocarbon adsorption, thereby limiting strongly adsorbed intermediates that are precursors to hydrogenolysis products and coke.

Keywords: Platinum-Tin, Bimetallics, Nanoclusters, H/D Exchange, C–H Activation, Isotopes

INTRODUCTION

There is an abundance of light paraffins in the world, and research to upgrade their value, for example by conversion to olefins or oxygenates, is of significant interest. Catalytic alkane dehydrogenation, a reaction that converts alkanes to olefins and H_2, is one conversion method that has been studied extensively,[1] and is commercially practiced. For example, UOP[2,3] uses a PtSn based catalyst supported on alumina in a process known as Oleflex, and Air Products/Houdry Division developed a chromium oxide based catalyst supported on alumina that is now licensed by CB&I Lummus, known as Catofin,[1] to produce light olefins such as propylene and isobutene. Many important factors go into catalytic dehydrogenation, including activity, selectivity, catalyst lifetime, and regenerability. Recently, a series of Pt and PtSn materials supported on purely siliceous MFI were reported,[4] in which subnanometric Pt or PtSn clusters were shown to form when K was introduced in the synthesis and the resultant materials (Pt-K/MFI and PtSn-K/MFI) were stable in both reducing and oxidizing conditions. The small particles give optimal atom economy,[5,6]

and their stability under oxidizing conditions may allow the material to be regenerated multiple times after it inevitably is deactivated by coke that is produced during a dehydrogenation reaction. For the PtSn-K/MFI material, additional work demonstrated that catalyst pre-treatment and specifically reduction temperature and time played a crucial role in modifying the material, where longer reduction times at 600 °C gave a catalyst that had increased stability and higher selectivity for propane dehydrogenation (PDH).[7]

It is well-known that Sn can modify Pt and has an effect on catalysis, which is why Sn is added. For example, one class of interactions is the formation of distinct PtSn alloys, which have significantly different adsorption, like low to zero H_2 chemisorptions, and poisoned catalytic properties.[8,9,10,11] Another class of PtSn interactions is when Pt interacts with an oxidized Sn species (e.g. "SnO"),[12,13,14,15,16] sometimes called and eggshell surface, and in these cases often high H_2 dispersions are observed with high catalytic activities. Notably, the structure of the bimetallic PtSn particles and the Pt-Sn interaction are also support dependent.[7,17,18,19,20,21,22] These interactions above are examples; however, it is important to note that there is a large range of the various types of interactions between Pt and Sn, and assessment of these interactions is not trivial. While these interactions are often broken down into either geometric or electronic effects, these categories are not mutually exclusive, and as the bimetallic particles get smaller, these effects become more interrelated. Most notably, with the smaller subnanometric particles (~0.5 nm) reported for PtSn-K/MFI,[4,7] characterization of these Pt-Sn interactions become even more difficult by more standard techniques (see below). Thus, we have implemented the use of the reactive characterizations, which indeed can differentiate the materials, and is discussed herein.

The PtSn-K/MFI material of focus here was previously characterized using techniques such as CO adsorption and FTIR spectroscopy, chemisorption, XANES, and EXAFS; it was proposed that the modification of catalytic performance was due to changes in the Pt-Sn interactions.[7] Several techniques, like Pt and Sn EXAFS were reported to be inconclusive for PtSn-K/MFI, and could not differentiate the materials based on reduction time. For example, the authors state: "In summary, neither the Pt LIII-edge nor the Sn K-edge EXAFS spectra show evidence of any kind of bimetallic interactions in this series of samples, in contrast to literature reports in which the two metals form well-established alloys."[7] Thus, Pt-Sn alloying is not indicated by EXAFS. Furthermore, although minor differences were observed with high resolution TEM imaging and FTIR spectroscopy, these techniques could not clearly identify substantial changes in the Pt-Sn interactions, or the formation of Pt-Sn alloys. While EXAFS has had significant impact and value in catalysis research, like any characterization technique, EXAFS has limitations and these have been reported,[23] often arising from structural heterogeneity.[24,25,26] Thus, the work detailed herein follows up on these aforementioned studies[4,7] and use reactive characterizations[27] to better understand the effect of reduction temperature on the catalytic results observed for alkane dehydrogenation.[28] The results of these reactive characterizations, and in particular H/D exchange to assess C–H activation, demonstrate their strong sensitivity to assess changes in catalyst performance.

RESULTS AND DISCUSSION

The PtSn-K/MFI sample was prepared according to the previous work (containing ~0.4 wt% Pt, 0.9 wt% Sn and 0.6 wt% K), which comprises subnanometric Pt clusters located in the 10R sinusoidal channels of MFI zeolite and atomically dispersed Sn species as extra-framework species, after being reduced by H_2 at

600 °C.[4,7] Two reduction times were studied in depth, 0 hr and 12 hr, both at 600 °C, and these materials are labeled as **PtSn-0hr** and **PtSn-12hr**, respectively. Additionally, a sample containing no Sn, i.e. Pt-K/MFI,[4] which is labeled as **Pt-only**, was also prepared and analyzed. It was previously postulated that during the course of a 12-hour reduction for PtSn-K/MFI, small amounts of Sn(IV) are reduced and incorporate/interact with the Pt particles, which modifies their catalytic behavior resulting in higher propylene selectivity for **PtSn-12hr**.[7] Higher propylene selectivity with **PtSn-12hr** is interpreted as decreasing the relative rate of hydrogenolysis compared to the rate of dehydrogenation.

Here, the reactivity of propane and H_2 at different H_2:propane ratios was studied on **PtSn-12hr** at 550 °C. These experiments were carried out in a well-mixed recirculating batch reactor, and the results are shown in Figure 1 (circles), where hydrocarbon partial pressures are shown as a function of time at different H_2:propane ratios. Analysis of the batch reactor results allow us to assess the rates of dehydrogenation and hydrogenolysis at a given process conditions. As can be seen in Figure 1, propylene formation (red) is significantly faster than the formation of cracked products (i.e. methane, ethane and ethylene, blue). The propylene yield decreases at higher H_2:propane ratios due to the decrease in thermodynamic equilibrium conversion.

Similar propane reactivity experiments were studied with **PtSn-0hr** at 550 °C, and these data are indicated in Figure 1 with stars. Several aspects to note are that: (i) the rate of propane conversion is faster on **PtSn-0hr**, as seen with the faster rate of disappearance of propane, (ii) the rate of dehydrogenation to form propylene is faster on **PtSn-0hr**, and (iii) the rate of hydrogenolysis is also faster on **PtSn-0hr**. Experiments in a plug-flow fixed bed reactor were also carried out at a large range of H_2:propane ratios, and are consistent with the observation of increased hyrogenolysis at constant residence time on **PtSn-0hr** (Figure S2). The observation of more facile hydrogenolysis with **PtSn-0hr** is indicative of stronger hydrocarbon adsorption, and thus weaker adsorption on **PtSn-12hr**, which is likely a consequence of the increased Pt-Sn interaction with longer reduction time. The propylene selectivity is a function of the relative rates of dehydrogenation and hydrogenolysis, and these selectivities are shown in Figure 2. Interestingly, it can be seen that at high H_2:propane ratios, the propylene selectivities are nearly identical and within the error of the experiments, indicating that reaction rates are more strongly controlled by H_2 adsorption rather than hydrocarbon adsorption under these conditions. PDH processes typically operate at lower H_2:propane ratios, and thus the higher propylene selectivity is relevant and important at these process conditions. The different propylene selectivities are consistent with the reported PDH results,[7] where lower reduction times give lower propylene selectivities for PDH.

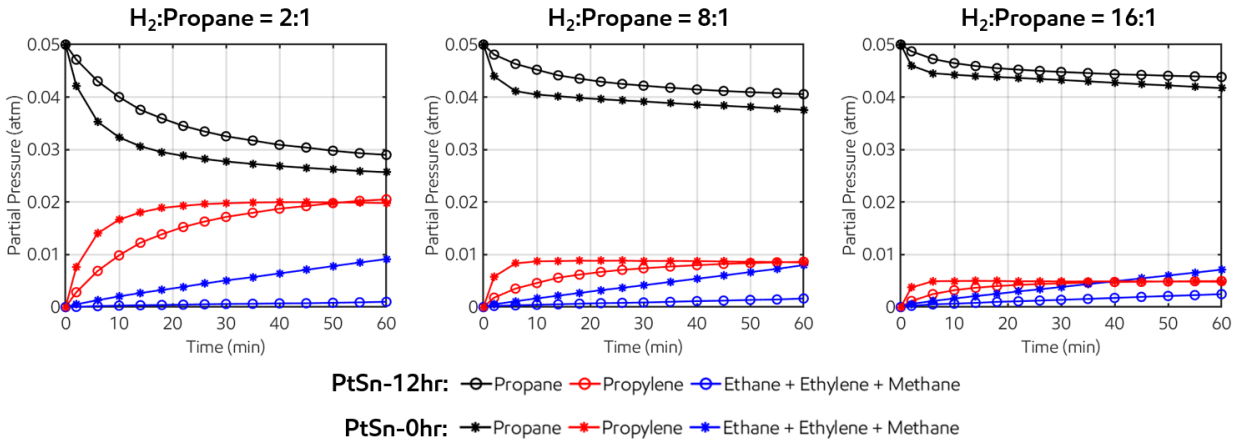

Figure 1. Propane reactivity on **PtSn-12hr** (circles) at **PtSn-0hr** (stars) at 550 °C, at varying H_2:propane ratios (left: 2:1, middle: 8:1, right: 16:1). Plots show hydrocarbon partial pressure (black: propane; red: propylene; blue: sum of ethane, ethylene and methane) as a function of time.

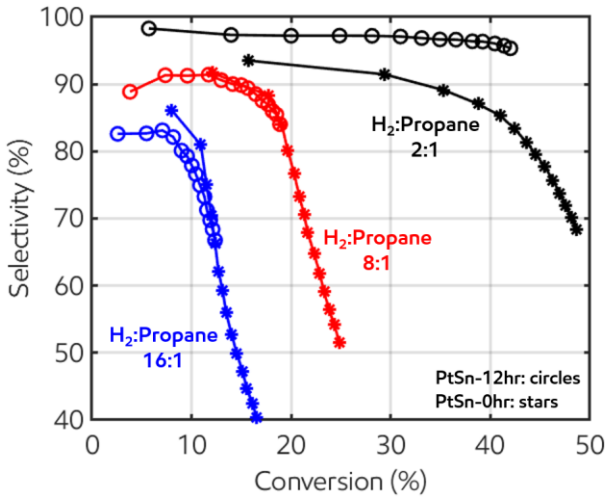

Figure 2. Selectivity towards PDH of **PtSn-12hr** (circles) and **PtSn-0hr** (stars) at varying H_2:propane ratios (black: 2:1, red: 8:1, blue: 16:1).

The Pt-only (i.e. no Sn) material (**Pt-only**), which was reduced at 600 °C for 1 hour, was also tested for its reactivity towards propane. Significant hydrogenolysis is observed for **Pt-only** at 450 °C, 100 °C lower than for the PtSn materials, as shown in Figure 3. For example, at a H_2:propane ratio of 2 (Figure 3, left), PDH and hydrogenolysis occur at similar rates on **Pt-only**. At 550 °C, hydrogenolysis rates are also comparable to PDH rates (Figure 4, left), resulting in low propylene selectivity (Figure 4, right). For comparison purposes, the three materials are plotted next to each in Figure 5, clearly demonstrating that the relative hydrogenolysis activity increases from **PtSn-12hr < PtSn-0hr << Pt-only** at low H_2:propane ratios.[29] These results clearly demonstrate that without Sn, hydrocarbon adsorption is significantly faster, resulting in high rates of hydrogenolysis.

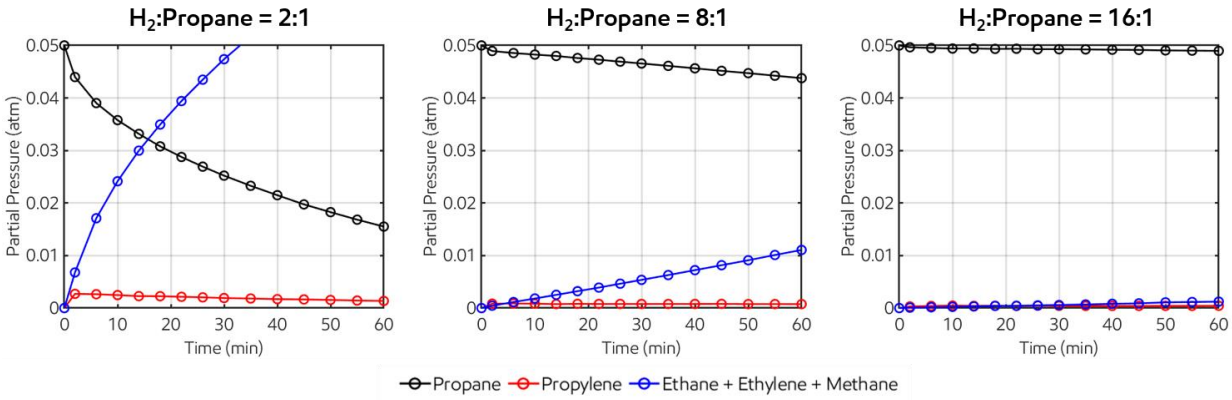

Figure 3. Propane reactivity on **Pt-only** at 450 °C, at varying H_2:propane ratios (left: 2:1, middle: 8:1, right: 16:1). Plots show hydrocarbon partial pressure (black: propane; red: propylene; blue: sum of ethane, ethylene and methane) as a function of time.

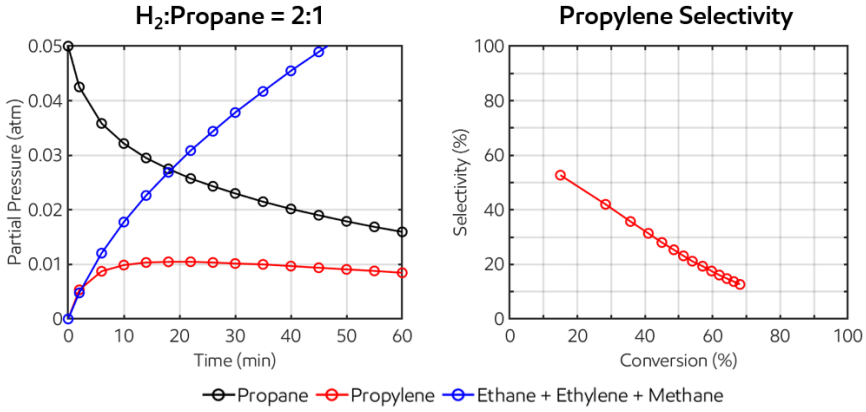

Figure 4. Propane reactivity on **Pt-only** at 550 °C at a H_2:propane ratio of 2:1. Plots show hydrocarbon partial pressure (black: propane; red: propylene; blue: sum of ethane, ethylene and methane) as a function of time (left), and propylene selectivity as a function of conversion (right).

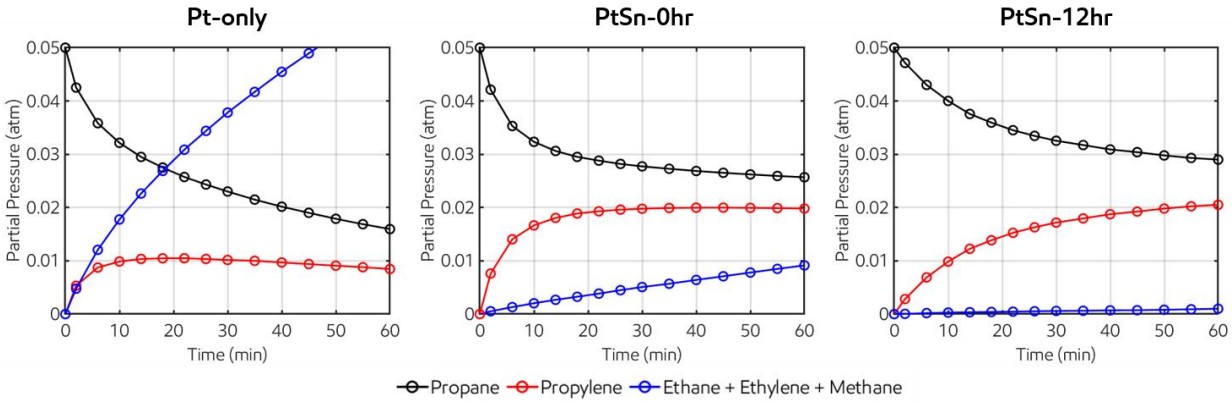

Figure 5. Side-by-side comparison of propane reactivity on **Pt-only**, **PtSn-0hr**, and **PtSn-12hr**, under the same process conditions (550 °C, 0.05 atm propane, 0.1 atm H_2, 5 mg catalyst).

Fixed-bed reactors studies were also conducted to confirm the observations in the well-mixed batch reactor, as batch-reactor studies for gas-phase dehydrogenation reactions are uncommon in the literature. The catalytic tests were performed at high space velocity at 600 °C in the absence of H_2 in the feed gas in

order to show the intrinsic activities of different types of species. As shown in Figure 6 (left), the **Pt-only** sample shows the highest initial conversion of propane while **PtSn-12hr** gives the lowest, which is consistent with the kinetic results shown in Figure 1. The initial selectivity to propylene obtained with the **Pt-only** sample is the lowest while the **PtSn-12hr** sample gives the highest selectivity (Figure 6, center). Consequently, the **PtSn-12hr** sample shows the slowest deactivation (Figure 6, right), and helps to support the conclusion that **PtSn-12hr** has weaker hydrocarbon adsorption, which not only limits hydrogenolysis, but also limits coke formation that causes deactivation, two reaction pathways that are often correlated based on requiring strong adsorption.

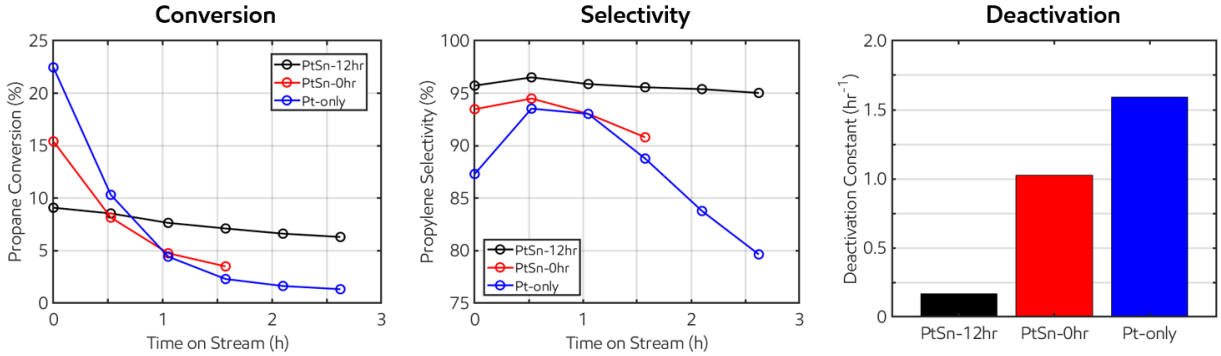

Figure 6. Catalytic results of **PtSn-12hr** (black), **PtSn-0hr** (red), and **Pt-only** (blue) sample in fixed-bed reactor for propane dehydrogenation. Reaction conditions: 5 mg catalyst, 20 mL/min propane and 60 mL/min N_2 as feed gas, 600 °C. The deactivation constants are obtained through the following formula: $\ln[(1 - X_{final})/X_{final}] = k_d \times T + \ln[(1 - X_{intial})/X_{intial}]$, where X_{final} and $X_{initial}$ are the final and initial propane conversions, respectively, T is the lifetime of the catalyst measured in the catalytic test (1.5 h) and k_d is the deactivation constant. The products were analyzed with online GC.

PDH necessarily involves C–H activation, as C–H bonds are broken to produce propylene, the study of C–H activation should be informative. We have previously shown that hydrogen/deuterium (H/D) exchange can serve as sensitive technique to differentiate Pt/SiO_2 catalysts that contain different levels of sodium,[30] and H/D exchange in alkanes has been studied extensively in general over many different metal catalysts.[31,32] Thus, **PtSn-0hr** and **PtSn-12hr** were studied for their C–H activation behavior by using H/D exchange. The experiments were carried out in the same well-mixed batch reactor, using mixtures of D_2 and ethane,[33] and the reactions were monitored by GC-MS (gas chromatography-mass spectrometry). Figure 7 and Figure 8 show individual H/D exchange experiments at several temperatures, on **PtSn-12hr** and **PtSn-0hr**, respectively, all at initial 20:1 D_2:ethane ratios.[34] It can clearly be seen that **PtSn-12hr** is slower to undergo H/D exchange than **PtSn-0hr**, at the same process conditions studied. These results indicate that **PtSn-0hr** more rapidly cleaves the C–H bond in ethane than **PtSn-12hr**, consistent with more Pt-Sn interactions in **PtSn-12hr** weakening its hydrocarbon adsorption kinetics and with the results above. Furthermore, we carried out a similar analysis as was done previously on a series of Pt/SiO_2 catalyst,[30,35] to assess the pressure dependences of ethane and D_2 for H/D exchange. These results indicate that C–H activation as assessed by H/D exchange are first order in ethane and negative first order for **PtSn-0hr** (Figure S3) and negative half order for **PtSn-12hr** (Figure S4) in D_2 (Table S1). A $PtSn/SiO_2$ catalyst,[36] in which an alloyed phased was confirmed by XRD (Figure S11), was tested for comparisons and showed a D_2 dependence of approximately –0.3, in addition to the higher temperature required to obtain similar

conversions. It is important to note that the pressure dependency experiments were conducted at different temperatures,[37] which can effect H (or D) coverage,[38] and thus the reaction orders in D_2 may also be affected by the difference in temperature. Nevertheless, the slower rates of H/D exchange at the same temperature and process conditions for **PtSn-12hr** indicate that the 12 hour reduction increases the interaction between Pt and Sn, thereby weakening hydrocarbon adsorption and C–H activation, and the trends in D_2 pressure dependency, albeit at different temperatures, are consistent with these results.

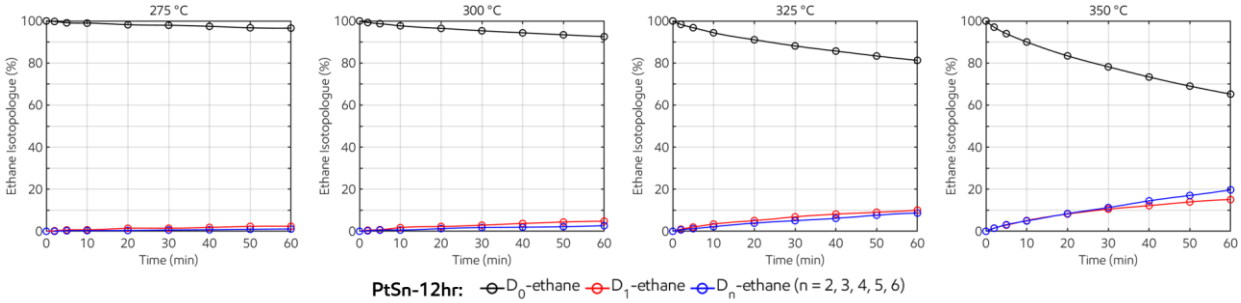

Figure 7. Monitoring H/D exchange between ethane and D_2 on **PtSn-12hr** at selected temperatures. C_2H_6 (black), C_2H_5D (red), sum of $C_2H_4D_2$, $C_2H_3D_3$, $C_2H_2D_4$, C_2HD_5 and C_2D_6 (blue).

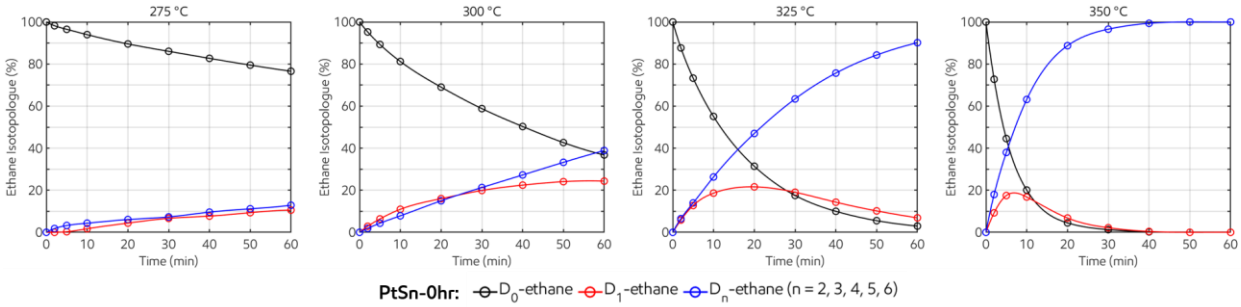

Figure 8. Monitoring H/D exchange between ethane and D_2 on **PtSn-0hr** at selected temperatures. C_2H_6 (black), C_2H_5D (red), sum of $C_2H_4D_2$, $C_2H_3D_3$, $C_2H_2D_4$, C_2HD_5 and C_2D_6 (blue).

The longer reduction time for **PtSn-12hr** increases the interaction between Pt and Sn, thereby inhibiting C–H activation, multiple exchange, and hydrogenolysis, resulting in higher selectivities towards dehydrogenation at the same process conditions as **PtSn-0hr**. Additional support for this hypothesis is obtained by examining the selectivity towards D_1-ethane, which occurs via stepwise exchange, versus the heavier isotopologues, D_{2+}-ethanes, which are produced by a combination of stepwise and multiple exchange (Figure S5). These selectivities are indicative of the relative rates of the first C–H activation and successive C–H activations when compared at constant conversion,[31] as depicted by a generic mechanistic representation of propane reactivity on a catalyst surface in Figure 9.[39] It can be seen that for **PtSn-0hr**, there is higher selectivity towards D_{2+}-ethanes (red) at constant conversion and temperature, indicating that the relative rate of the second C–H activation compared with the first is greater than with **PtSn-12hr**. The greater propensity for multiple exchange has been proposed to be a consequence of the adsorption strength of the hydrocarbon on the metal surface, where more strongly adsorbed species will undergo multiple exchange.[31,40,41] Strongly adsorbed species (a.k.a. deep dehydrogenation) which are heavily dehydrogenated are also proposed as intermediates that lead to hydrogenolysis,[29] and coke, as shown in

Figure 9. Thus, it is postulated that the longer reduction time for **PtSn-12hr** increases the interaction between Pt and Sn, thereby inhibiting C–H activation, multiple exchange, and hydrogenolysis, resulting in higher selectivities towards dehydrogenation at the same process conditions as **PtSn-0hr**.

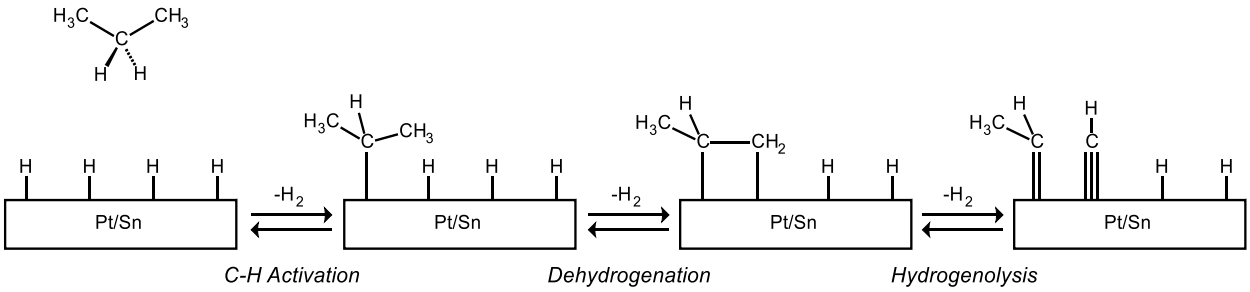

Figure 9. Mechanism of successive C–H activations and C–C activation.

To further confirm the relevance of C–H activation during PDH, isotope experiments under PDH conditions were tested. A 1:1 mixture of C_3H_8 and C_3D_8 (0.1 atm each, no H_2 added) was allowed to react on **PtSn-12hr** at 550 °C.[42] The reaction progress was analyzed by GC coupled with both a MS and FID (flame ionization detector); the GC-FID chromatogram is shown in Figure S6, which clearly demonstrates the disappearance of propane and appearance of propylene. Notably, the isotopologues of propane, C_3H_8 and C_3D_8, can be separated, shown in Figure S7. It can be seen that C_3H_8 reacts faster than C_3D_8, based on the faster disappearance of C_3H_8 in the GC, and integration of the chromatogram gives the reaction progress plot shown in Figure 10. Based on the initial rates of disappearance of C_3H_8 and C_3D_8, an observed normal kinetic isotope effect (KIE) of ~2.5. was obtained.

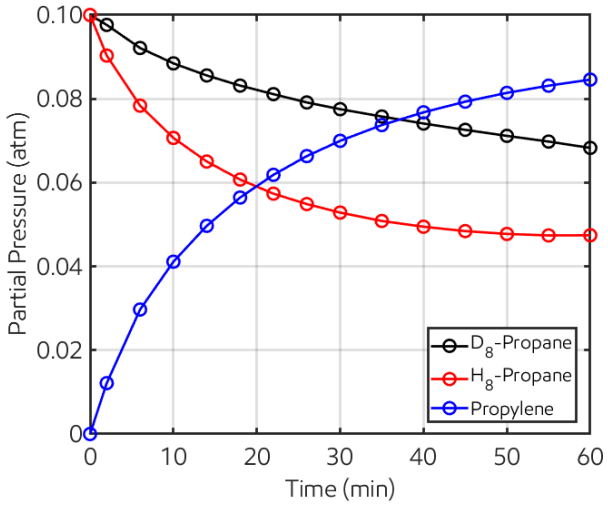

Figure 10. Reaction progress of reaction of 1:1 mixture of C_3H_8 (H_8-propane) and C_3D_8 (D_8-propane) on **PtSn-12hr** (black: D_8-propane; red: H_8-propane; blue: propylene).

Additional information is obtained by analysis of the mass spectra during the course of the PDH reaction. The mass spectra of C_3H_8, C_3D_8, C_3H_6 and C_3D_6 are shown in Figure S8.[43] The mass spectra of the

pure isotopologues are useful as a source of comparison when analyzing the mass spectra of the gas-phase mixture (1:1 mixture of C_3H_8 and C_3D_8 at time zero) over the course of the reaction on **PtSn-12hr** at 550 °C, in order to assess where C–H activation is occurring; these spectra are shown in Figure S9. There is little isotope exchange between the propane isotopologues (i.e. C_3H_8 and C_3D_8) during early reaction times, based on the chromatogram analysis, showing well-defined separation between C_3H_8 and C_3D_8. At later times, the two signals merge, indicating isotopic scrambling between propane isotopologues, and is further confirmed by analysis of the mass spectra (Figure S9). In contrast, the propylene exists as a mixture of isotopologues at all times, and shifts more towards deuterated propylene with time, due to the KIE observed above, where less C_3D_8 is reactive than C_3H_8 at early times. These results together indicate that C–H activation is rate limiting during PDH, and experimentally irreversible at early times, which is consistent with previously reported results for dehydrogenation.[44,45]

CONCLUSIONS

In conclusion, PtSn-K/MFI, which contains subnanometric PtSn particles inside MFI, is a highly active and selective catalyst for PDH. Increased reduction time at 600 °C modifies the material, to increase its selectivity and limit catalyst deactivation during PDH catalysis. This modification is proposed to be due to changes in the interactions between Pt and Sn, where longer reduction times increases their bimetallic interactions, while not forming a PtSn alloy, and gives superior catalytic properties. Specifically, the increased interaction in **PtSn-12hr** compared to **PtSn-0hr** causes a slight decrease in the general adsorption strength of the hydrocarbon species on the surface of the subnanometric clusters, which thereby limits the rate of both hydrogenolysis and coking. These modifications are minor enough, such that they were not observed by state-of-the-art characterization techniques like EXAFS and TEM,[7] but are readily seen by reactive characterizations, such as H/D exchange, highlighting the strong sensitivity reactive characterizations can have. These findings demonstrate the substantial effect that minor interactions can cause on hydrocarbon catalysis.

ACKNOWLEDGMENTS

Trong Pham and Gene Terefenko are thanked for assistance with materials synthesis and helpful discussion. Thanks to Stu Soled, Sal Miseo and Randall Meyer for helpful discussion. The reviewer is thanked for helpful comments and suggestions.

REFERENCES

(1) Sattler, J. J. H. B.; Ruiz-Martinez, J.; Santillan-Jimenez, E.; Weckhuysen, B. M. Catalytic Dehydrogenation of Light Alkanes on Metals and Metal Oxides *Chem. Rev.* **2014**, *114*, 10613-10653.

(2) Imai, T.; Abrevaya, H.; Bricker, J. C.; Jan, D.-Y. US Patent, 4,827,072, 1989.

(3) Imai, T.; Bricker, J. C. US Patent, 4,652,687, 1987.

(4) Liu, L. C.; Lopez-Haro, M.; Lopes, C. W.; Li, C. G.; Concepcion, P.; Simonelli, L.; Calvino, J. J.; Corma, A. Regioselective generation and reactivity control of subnanometric platinum clusters in zeolites for high-temperature catalysis *Nature Materials* **2019**, *18*, 866-783.

(5) Liu, L. C.; Corma, A. Metal Catalysts for Heterogeneous Catalysis: From Single Atoms to Nanoclusters and Nanoparticles *Chem. Rev.* **2018**, *118*, 4981-5079.

(6) For related work on PtZn on MFI, see: (a) Wang, Y.; Hu, Z.-P.; Lv, X.; Chen, L.; Yuan, Z.-Y. Ultrasmall PtZn bimetallic nanoclusters encapsulated in silicalite-1 zeolite with superior performance for propane dehydrogenation *J. Catal.* **2020**, *385*, 61-69.
(b) Sun, Q.; Wang, N.; Fan, Q.; Zeng, L.; Mayoral, A.; Miao, S.; Yang, R.; Jiang, Z.; Zhou, W.; Zhang, J.; Zhang, T.; Xu, J.; Zhang, P.; Cheng, J.; Yang, D.-C.; Jia, R.; Li, L.; Zhang, Q.; Wang, Y.; Terasaki, O.; Yu, J. Subnanometer Bimetallic Pt-Zn Clusters in Zeolites for Propane Dehydrogenation *Angew. Chem. Int. Ed.* **2020**, *59*, 19450-19459.

(7) Liu, L. C.; Lopez-Haro, M.; Lopes, C. W.; Rojas-Buzo, S.; Concepcion, P.; Manzorro, R.; Simonelli, L.; Sattler, A.; Serna, P.; Calvino, J. J.; Corma, A. Structural Modulation and Direct Measurement of Subnanometric Bimetallic PtSn Clusters Confined in Zeolites, *Nature Catalysis*, **2020**, *3*, 628-638.

(8) Verbeek, H.; Sachtler, W. M. H. The study of the alloys of platinum and tin by chemisorption *J. Catal.* **1976**, *42*, 257-267.

(9) Dautzenberg, F. M.; Helle, J. N.; Biloen, P.; Sachtler, W. M. H. Conversion of n-hexane over monofunctional supported and unsupported PtSn catalysts *J. Catal.* **1980**, *63*, 119-128.

(10) Sexton, B. A.; Hughes, A. E.; Foger, K. An X-ray photoelectron spectroscopy and reaction study of Pt-Sn catalysts *J. Catal.* **1984**, *88*, 466-477.

(11) (a) Srinivasan, R.; Davis, B. H. Paraffin dehydrocyclization. Part 9. Conversion of n-octane with Pt-Sn catalysts at atmospheric pressure *J. Mol. Catal.* **1994**, *88*, 343-358.
(b) Sparks, D. E.; Srinivasan, R.; Davis, B. H. Paraffin dehydrocyclization. Part 10. Conversion of n-octane with supported Pt-Sn catalysts at 100 psig *J. Mol. Catal.* **1994**, *88*, 359-376.

(12) Burch, R. Platinum-tin reforming catalysts: I. The oxidation state of tin and the interaction between platinum and tin *J. Catal.* **1981**, *71*, 348-359.

(13) Lieske, H.; Völter, J. State of tin in Pt-SnAl2O3 reforming catalysts investigated by TPR and chemisorption *J. Catal.* **1984**, *90*, 96-105.

(14) Bacaud, R.; Bussière, P.; Figueras, F. Mössbauer spectra investigation of the role of tin in platinum-tin reforming catalysts *J. Catal.* **1981**, *69*, 399-409.

(15) Metallic tin on alumina was observed by Mössbauer spectroscopy at higher tin loadings. See: Li, Y.-X.; Klabunde, K. J.; Davis, B. H. Alloy formation in supported Pt-Sn catalysts: Mossbauer studies *J. Catal.* **1991**, *128*, 1-12.

(16) Adkins, S. R.; Davis, B. H. The chemical state of tin in platinum-tin-alumina catalysts *J. Catal.* **1984**, *89*, 371-379.

(17) Cortright, R. D.; Dumesic, J. A. Microcalorimetric, Spectroscopic, and Kinetic Studies of Silica Supported Pt and Pt/Sn Catalysts for Isobutane Dehydrogenation *J. Catal.* **1994**, *148*, 771-778.

(18) Cortright, R. D.; Dumesic, J. A. Effects of potassium on silica-supported Pt and Pt/Sn catalysts for isobutane dehydrogenation *J. Catal.* **1995**, *157*, 576-583.

(19) Cortright, R. D.; Dumesic, J. A. L-zeolite-supported platinum and platinum/tin catalysts for isobutane dehydrogenation *App. Catal. A* **1995**, *129*, 101-115.

(20) Meitzner, G.; Via, G. H.; Lytle, F. W.; Fung, S. C.; Sinfelt, J. H. Extended x-ray absorption fine-structure studies of platinum tin catalysts *J. Phys. Chem.* **1988**, *92*, 2925-2932.

(21) Resasco, D. E. 2002 Dehydrogenation – Heterogeneous. In Encyclopedia of Catalysis, I. Horváth (Ed.).

(22) Virnovskaia, A.; Morandi, S.; Rytter, E.; Ghiotti, G.; Olsbye, U. Characterization of Pt,Sn/Mg(Al)O catalysts for light alkane dehydrogenation by FT-IR Spectroscopy and catalytic measurements *J. Phys. Chem. C* **2007**, *111*, 14732-14742.

(23) Feng, K.; Zhang, H.; Gao, J.; Xu, J.; Dong, Y.; Kang, Z.; Zhong, J. Single atoms or not? The limitation of EXAFS *Appl. Phys. Lett.* **2020**, *116*, 191903.

(24) Nowicka, E.; Althahban, S. M.; Luo, Y.; Kriegel, R.; Shaw, G.; Morgan, D. J.; He, Q.; Watanabe, M.; Armbrüster, M.; Kiely, C. J.; Hutchings, G. J. Highly selective PdZn/ZnO catalysts for the methanol steam reforming reaction *Catal. Sci. Technol.* **2018**, *8*, 5848-5857.

(25) Timoshenko, J.; Jeon, H. S.; Sinev, I.; Haase, F. T.; Herzog, A.; Roldan Cuenya, B. Linking the evolution of catalytic properties and structural changes in copper–zinc nanocatalysts using operando EXAFS and neural-networks *Chem. Sci.* **2020**, *11*, 3727-3736.

(26) Timoshenko, J.; Roldan Cuenya, B. In Situ/Operando Electrocatalyst Characterization by X-ray Absorption Spectroscopy *Chem. Rev.* **2021**, *121*, 882-961.

(27) For previous examples of reactive characterizations, see:
(a) Larsen, G.; Haller, G. L. Metal-support effects in Pt/L-zeolite catalysts *Catal. Lett.* **1989**, *3*, 103-110.
(b) Larsen, G.; Haller, G. L. Characterization of Pt/L-Zeolite Catalysts by Chemisorption, EXAFS and Reaction of Neopentane with H_2 *Catal. Today* **1992**, *15*, 431-442.

(28) The benefit of coupling EXAFS and reactivity studies has been noted previously. For example, see: Zeng, S.; Shan, S.; Lu, A.; Wang, S.; Caracciolo, D. T.; Robinson, R. J.; Shang, G.; Xue, L.; Zhao, Y.; Zhang, A.; Liu, Y.; Liu, S.; Liu, Z.; Bai, F.; Wu, J.; Wang, H.; Zhong, C.-J. Copper-alloy catalysts: structural characterization and catalytic synergies *Catal. Sci. Technol.* **2021**, *11*, 5712-5733.

(29) For alkane hydrogenolysis and the effect of H_2:hydrocarbon ratio, see:
(a) Flaherty, D. W.; Iglesia, E. Transition-State Enthalpy and Entropy Effects on Reactivity and Selectivity in Hydrogenolysis of n-Alkanes *J. Am. Chem. Soc.* **2013**, *135*, 18586-18599.
(b) Flaherty, D. W.; Uzun, A.; Iglesia, E. Catalytic Ring Opening of Cycloalkanes on Ir Clusters: Alkyl Substitution Effects on the Structure and Stability of C-C Bond Cleavage Transition States *J. Phys. Chem. C* **2015**, *119*, 2597-2613.

(30) Sattler, A.; Paccagnini, M.; Lanci, M. P.; Miseo, S.; Kliewer, C. E. Platinum Catalyzed C–H Activation and the Effect of Metal–Support Interactions *ACS Catalysis* **2020**, *10*, 710-720.

(31) For reviews, see:
(a) Sattler, A. Hydrogen/Deuterium (H/D) Exchange Catalysis in Alkanes *ACS Catal.* **2018**, *8*, 2296-2312.
(b) Kemball, C. The Catalytic Exchange of Hydrocarbons with Deuterium *Adv. Catal.* **1959**, *11*, 223-262.
(c) Kemball, C. Chemical Processes On Heterogeneous Catalysts *Chem. Soc. Rev.* **1984**, *13*, 375-392.

(d) Burwell, R. L. Deuterium as a tracer in reactions of hydrocarbons on metallic catalysts *Acc. Chem. Res.* **1969**, *2*, 289-296.

(32) For H/D exchange studies on alkane aromatization, see:
(a) Shi, B. C.; Davis, B. H. Deuterium Tracer Study of The Conversion of Methylcyclohexane N-Octane Mixtures With Pt/SiO_2 And Pt/Al_2O_3 Catalysts *J. Catal.* **1994**, *147*, 38-47.
(b) Shi, B. C.; Davis, B. H. Reaction pathway for alkane dehydrocyclization *J. Catal.* **1996**, *162*, 134-137.
(c) Wang, Y. G.; Shi, B. C.; Guthrie, R. D.; Davis, B. H. Paraffin dehydrocyclization: Isotope effect and competitive conversion of alkane/naphthene mixture with a Pt-Mg(Al) oxide catalyst *J. Catal.* **1997**, *170*, 89-95.
(d) Shi, B. C.; Davis, B. H. Dehydrocyclization of n-octane: Role of alkene intermediates in the reaction mechanism *J. Catal*. **1997**, *168*, 129-132.
(e) Shi, B. C.; Davis, B. H. The kinetic isotope effect for alkane dehydrocyclization *11th International Congress on Catalysis - 40th Anniversary* **1996**, *101*, 1145-1154.

(33) Ethane was used instead of propane because the mass spectra of each ethane isotopologue and isotopomer have been determined, and allow for deconvolution and kinetics analysis.

(34) High D_2:ethane ratios are used such that upon C–H activation, the reverse step will be statistically more likely to form a C–D bond.

(35) For additional experiments examining ethane and D_2 dependences on Pt catalysts, see: Loaiza, A.; Xu, M. D.; Zaera, F. On the mechanism of the H-D exchange reaction in ethane over platinum catalysts *J. Catal.* **1996**, *159*, 127-139.

(36) The $PtSn/SiO_2$ sample was made by wet impregnation, using $Pt(NH_3)_4(NO_3)_2$ and $SnCl_2$ (1:2 Pt:Sn molar ratio), which was dried at 100 °C, calcined at 350 °C, and then reduced at 450 °C prior to H/D exchange experiments. XRD analysis demonstrated the majority of Pt was present at PtSn, with a small amount of Pt present (see Supporting Information). Previous results show that Pt alone has an inverse first order dependence on D_2 (Reference 30), and the minor Pt component was de-edged by feeding methane for 2 hours prior to H/D exchange experiments.

(37) Experiments were conducted at similar reaction rates (see Figures S2 – S4) rather than the same temperature, due to experimental limitations. For example, at 325 °C, **PtSn-0hr** H/D exchange is rapid (see Figure 8), and obtaining rate differences at different ethane and D_2 partial pressure is experimentally unreliable. Additionally, at 325 °C, $PtSn/SiO_2$ was found to be inactive for H/D exchange, thus not allowing for the measurement of ethane and D_2 pressure dependencies.

(38) Garcia-Dieguez, M.; Hibbitts, D. D.; Iglesia, E. Hydrogen Chemisorption Isotherms on Platinum Particles at Catalytic Temperatures: Langmuir and Two-Dimensional Gas Models Revisited *J. Phys. Chem. C* **2019**, *123*, 8447-8462.

(39) For DFT studies on propane dehydrogenation, see: Xiao, L.; Shan, Y.-L.; Sui, Z.-J.; Chen, D.; Zhou, X.-G.; Yuan, W.-K.; Zhu, Y.-A. *ACS Catal.* **2020**, *10*, 14887-14902.

(40) Anderson, J. R.; Kemball, C. Catalysis on evaporated metal films .3. The efficiency of different metals for the reaction between ethane and deuterium *Proc. Roy. Soc. A* **1954**, *223*, 361-377.

(41) Kemball, C. Catalysis on evaporated metal films .4. Exchange between propane and deuterium and isobutane and deuterium *Proc. Roy. Soc. A* **1954**, *223*, 377-392.

(42) A 1:1 mixture was used such that (i) the rates of C_3H_8 and C_3D_8 disappearance could be obtained under identical conditions, and removes the error of small changes in catalyst loading and temperature when running consecutive experiments, and (ii) such that isotope exchange to assess the relative rates of a single C–H activation versus multiple C–H activations could be obtained. Separate experiments with only C_3H_8 and C_3D_8 were also conducted, and show similar KIEs.

(43) The mass spectra of C_3D_6 was obtained by dehydrogenation of C_3D_8 in the presence of D_2.

(44) Virnovskaia, A.; Rytter, E.; Olsbye, U. Kinetic and isotopic study of ethane dehydrogenation over a semicommercial Pt,Sn/Mg(Al)O catalyst *Ind. Eng. Chem. Res.* **2008**, *47*, 7167-7177.

(45) Cortright, R. D.; Levin, P. E.; Dumesic, J. A. Kinetic studies of isobutane dehydrogenation and isobutene hydrogenation over Pt/Sn-based catalysts *Ind. Eng. Chem. Res.* **1998**, *37*, 1717-1723.